Robust Resource Allocation with Joint Carrier Aggregation for Multi-Carrier Cellular Networks

Haya Shajaiah, Ahmed Abdelhadi, and T. Charles Clancy
Bradley Department of Electrical and Computer Engineering
Hume Center, Virginia Tech, Arlington, VA, 22203, USA
{hayajs, aabdelhadi, tcc}@vt.edu

Abstract—In this paper, we present a novel approach for robust optimal resource allocation with joint carrier aggregation to allocate multiple carriers resources optimally among users with elastic and inelastic traffic in cellular networks. We use utility proportional fairness allocation policy, where the fairness among users is in utility percentage of the application running on the user equipment (UE). Each UE is assigned an application utility function based on the type of its application. Our objective is to allocate multiple carriers resources optimally among users subscribing for mobile services. In addition, each user is guaranteed a minimum quality of service (QoS) that varies based on the user's application type. We present a robust algorithm that solves the drawback in the algorithm presented in [1] by preventing the fluctuations in the resource allocation process, in the case of scarce resources, and allocates optimal rates for both high-traffic and low-traffic situations. Our distributed resource allocation algorithm allocates an optimal rate to each user from all carriers in its range while providing the minimum price for the allocated rate. In addition, we analyze the convergence of the algorithm with different network traffic densities and show that our algorithm provides traffic dependent pricing for network providers. Finally, we present simulation results for the performance of our resource allocation algorithm.

Index Terms—Optimal Resource Allocation; Joint Carrier Aggregation; Utility Proportional Fairness; Elastic Traffic, Inelastic Traffic

I. INTRODUCTION

In recent years, the number of mobile subscribers and their traffic have increased rapidly. Mobile subscribers are currently running multiple applications, simultaneously, on their smart phones that require a higher bandwidth and make users so limited to the carrier resources. Network providers are now offering multiple services such as multimedia telephony and mobile-TV [2]. More spectrum is required to meet these demands [3]. However, it is difficult to provide the required resources with a single frequency band due to the scarcity of the available radio spectrum. Therefore, aggregating different carriers' frequency bands is needed to utilize the radio resources across multiple carriers and allow a scalable expansion

of the effective bandwidth delivered to the user terminal, leading to interband non-contiguous carrier aggregation [4].

Carrier aggregation (CA) is one of the most distinct features of 4G systems including Long Term Evolution Advanced (LTE Advanced). Given the fact that LTE requires wide carrier bandwidths to utilize such as 10 and 20 MHz, CA needs to be taken into consideration when designing the system to overcome the spectrum scarcity challenges. With the CA being defined in [5], two or more component carriers (CCs) of the same or different bandwidths can be aggregated to achieve wider transmission bandwidths between the evolve node B (eNodeB) and the UE. An overview of CA framework and cases is presented in [6]. Many operators are willing to add the CA feature to their plans across a mixture of macro cells and small cells. This will provide capacity and performance benefits in areas where small cell coverage is available while enabling network operators to provide robust mobility management on their macro cell networks.

Increasing the utilization of the existing spectrum can significantly improve network capacity, data rates and user experience. Some spectrum holders such as government users do not use their entire allocated spectrum in every part of their geographic boundaries most of the time. Therefore, the National Broadband Plan (NBP) and the findings of the President's Council of Advisors on Science and Technology (PCAST) spectrum study have recommended making the under-utilized federal spectrum available for secondary use [7]. Spectrum sharing enables wireless systems to harvest under-utilized swathes of spectrum, which would vastly increase the efficiency of spectrum usage. Making more spectrum available can provide significant gain in mobile broadband capacity only if those resources can be aggregated efficiently with the existing commercial mobile system resources.

This non-contiguous carrier aggregation task is a challenging. The challenges are both in hardware implementation and joint optimal resource allocation. Hardware implementation challenges are in the need for multiple oscillators, multiple RF chains, more powerful signal processing, and longer battery life [8]. In order to allocate different carriers resources optimally among mobile users in their coverage areas, a distributed resource allocation algorithm between the UEs and the eNodeBs is needed.

A multi-stage resource allocation (RA) with carrier aggregation algorithms are presented in [9]–[11]. The algorithm in [9] uses utility proportional fairness approach to allocate the

primary and the secondary carriers resources optimally among mobile users in their coverage area. The primary carrier first allocates its resources optimally among users in its coverage area. The secondary carrier then starts allocating optimal rates to users in its coverage area based on the users applications and the rates allocated to them by the primary carrier. A RA with CA optimization problem is presented in [10] to allocate resources from the LTE Advanced carrier and the MIMO radar carrier to each UE, in a LTE Advanced cell based on the application running on the UE. A price selective centralized RA with CA algorithm is presented in [11] to allocate multiple carriers resources optimally among users while giving the user the ability to select one of the carriers to be its primary carrier and the others to be its secondary carriers. The UE's decision is based on the carrier price per unit bandwidth. However, the multi-stage RA with CA algorithms presented in [9]–[11] guarantee optimal rate allocation but not optimal pricing.

In this paper, we focus on solving the problem of utility proportional fairness optimal RA with joint CA for multi-carrier cellular networks. The RA with joint CA algorithm presented in [1] fails to converge for high-traffic situations due to the fluctuation in the RA process. In this paper, we present a robust algorithm that solves the drawbacks in [1] and allocates multiple carriers resources optimally among UEs in their coverage area for both high-traffic and low-traffic situations. Additionally, our proposed distributed algorithm outperforms the multi-stage RA with CA algorithms presented in [9]–[11] as it guarantees that mobile users are assigned optimal (minimum) price for resources. We formulate the multi-carrier RA with CA optimization problem into a convex optimization framework. We use logarithmic and sigmoidal-like utility functions to represent delay-tolerant and real-time applications, respectively, running on the mobile users' smart phones [12]. Our model supports both contiguous and non-contiguous carrier aggregation from one or more network providers. During the resource allocation process, our distributed algorithm allocates optimal resources from one or more carriers to provide the lowest resource price for the mobile users. In addition, we use a utility proportional fairness approach that ensures non-zero resource allocation for all users and gives real-time applications priority over delay-tolerant applications due to the nature of their applications that require minimum encoding rates.

A. Related Work

There has been several works in the area of resource allocation optimization to utilize the scarce radio spectrum efficiently. The authors in [13]–[16] have used a strictly concave utility function to represent each user's elastic traffic and proposed distributed algorithms at the sources and the links to interpret the congestion control of communication networks. Their work have only focussed on elastic traffic and did not consider real-time applications as it have non-concave utility functions as shown in [17]. The authors in [18] and [19] have argued that the utility function, which represents the user application performance, is the one that needs to be shared fairly rather than the bandwidth. In this

paper, we consider using resource allocation to achieve a utility proportional fairness that maximizes the user satisfaction. If a bandwidth proportional fairness is applied through a max-min bandwidth allocation, users running delay-tolerant applications receive larger utilities than users running real-time applications as real-time applications require minimum encoding rates and their utilities are equal to zero if they do not receive their minimum encoding rates.

The proportional fairness framework of Kelly introduced in [13] does not guarantee a minimum QoS for each user application. To overcome this issue, a resource allocation algorithm that uses utility proportional fairness policy is introduced in [12]. We believe that this approach is more appropriate as it respects the inelastic behavior of real-time applications. The utility proportional fairness approach in [12] gives real-time applications priority over delay tolerant applications when allocating resources and guarantees that no user is allocated zero rate. In [12], [20] and [21], the authors have presented optimal resource allocation algorithms to allocate single carrier resources optimally among mobile users. However, their algorithms do not support multi-carrier resource allocation. To incorporate the carrier aggregation feature, we have introduced a multi-stage resource allocation using carrier aggregation in [9]. In [22] and [23], we present resource allocation with users discrimination algorithms to allocate the eNodeB resources optimally among mobile users with elastic and inelastic traffic. In [24], the authors have presented a radio resource block allocation optimization problem using a utility proportional fairness approach. The authors in [25] have presented an application-aware resource block scheduling approach for elastic and inelastic adaptive real-time traffic where users are assigned to resource blocks.

On the other hand, resource allocation for single cell multi-carrier systems have been given extensive attention in recent years [26]–[28]. In [29]–[32], the authors have represented this challenge in optimization problems. Their objective is to maximize the overall cell throughput with some constraints such as fairness and transmission power. However, transforming the problem into a utility maximization framework can achieve better users satisfaction rather than better system-centric throughput. Also, in practical systems, the challenge is to perform multi-carrier radio resource allocation for multiple cells. The authors in [33], [34] suggested using a distributed resource allocation rather than a centralized one to reduce the implementation complexity. In [35], the authors propose a collaborative scheme in a multiple base stations (BSs) environment, where each user is served by the BS that has the best channel gain with that user. The authors in [36] have addressed the problem of spectrum resource allocation in carrier aggregation based LTE Advanced systems, with the consideration of UEs MIMO capability and the modulation and coding schemes (MCSs) selection.

B. Our Contributions

Our contributions in this paper are summarized as:
- We consider the RA optimization problem with joint CA presented in [1] that uses utility proportional fairness

approach and solves for logarithmic and sigmoidal-like utility functions representing delay-tolerant and real-time applications, respectively.

- We prove that the optimization problem is convex and therefore the global optimal solution is tractable. In addition, we present a robust distributed resource allocation algorithm to solve the optimization problem and provide optimal rates in high-traffic and low-traffic situations.
- Our proposed algorithm outperforms that presented in [1] by preventing the fluctuations in the RA process when the resources are scarce with respect to the number of users. It also outperforms the algorithms presented in [9]–[11] as it guarantees that mobile users receive optimal price for resources.
- We present simulation results for the performance of our RA algorithm and compare it with the performance of the multi-stage RA algorithm presented in [9]–[11].

The remainder of this paper is organized as follows. Section II presents the problem formulation. Section III proves that the global optimal solution exists and is tractable. In Section IV, we discuss the conversion of the primal optimization problem into a dual problem. Section V presents our distributed resource allocation algorithm with joint carrier aggregation for the utility proportional fairness optimization problem. In Section VI, we present convergence analysis for the allocation algorithm and a modification for robustness at peak-traffic hours. In section VII, we discuss simulation setup, provide quantitative results along with discussion and compare the performance of the proposed algorithm with the one presented in [9]–[11]. Section VIII concludes the paper.

II. PROBLEM FORMULATION

We consider LTE mobile system consisting of K carriers eNodeBs with K cells and M UEs distributed in these cells. The rate allocated by the lth carrier eNodeB to i^{th} UE is given by r_{li} where $l = \{1, 2, ..., K\}$ and $i = \{1, 2, ..., M\}$. Each UE has its own utility function $U_i(r_{1i} + r_{2i} + ... + r_{Ki})$ that corresponds to the type of traffic being handled by the ith UE. Our objective is to determine the optimal rates that the lth carrier eNodeB should allocate to the nearby UEs. We express the user satisfaction with its provided service using utility functions that represent the degree of satisfaction of the user function with the rate allocated by the cellular network [37] [17] [38]. We assume the utility functions $U_i(r_{1i} + r_{2i} + ... + r_{Ki})$ to be a strictly concave or a sigmoidal-like functions. The utility functions have the following properties:

- $U_i(0) = 0$ and $U_i(r_{1i} + r_{2i} + ... + r_{Ki})$ is an increasing function of r_{li} for l.
- $U_i(r_{1i} + r_{2i} + ... + r_{Ki})$ is twice continuously differentiable in r_{li} for all l.

In our model, we use the normalized sigmoidal-like utility function, as in [37], that can be expressed as

$$U_i(r_{1i} + r_{2i} + ... + r_{Ki}) = c_i \Big(\frac{1}{1 + e^{-a_i(\sum_{l=1}^{K} r_{li} - b_i)}} - d_i \Big) \quad (1)$$

where $c_i = \frac{1 + e^{a_i b_i}}{e^{a_i b_i}}$ and $d_i = \frac{1}{1 + e^{a_i b_i}}$. So, it satisfies $U_i(0) = 0$ and $U_i(\infty) = 1$. We use the normalized logarithmic utility

function, as in [38], that can be expressed as

$$U_i(r_{1i} + r_{2i} + ... + r_{Ki}) = \frac{\log(1 + k_i \sum_{l=1}^{K} r_{li})}{\log(1 + k_i r_{max})} \quad (2)$$

where r_{max} is the required rate for the user to achieve 100% utility percentage and k_i is the rate of increase of utility percentage with allocated rates. So, it satisfies $U_i(0) = 0$ and $U_i(r_{max}) = 1$. We consider the utility proportional fairness objective function that is given by

$$\max_{\mathbf{r}} \prod_{i=1}^{M} U_i(r_{1i} + r_{2i} + ... + r_{Ki}) \quad (3)$$

where $\mathbf{r} = \{\mathbf{r}_1, \mathbf{r}_2, ..., \mathbf{r}_M\}$ and $\mathbf{r}_i = \{r_{1i}, r_{2i}, ..., r_{Ki}\}$. The goal of this resource allocation objective function is to maximize the total system utility while ensuring proportional fairness between utilities (i.e., the product of the utilities of all UEs). This resource allocation objective function inherently guarantees:

- non-zero resource allocation for all users. Therefore, the corresponding resource allocation optimization problem provides a minimum QoS for all users.
- priority to users with real-time applications. Therefore, the corresponding resource allocation optimization problem improves the overall QoS for LTE system.

The basic formulation of the utility proportional fairness resource allocation problem is given by the following optimization problem:

$$
\begin{aligned}
\max_{\mathbf{r}} \quad & \prod_{i=1}^{M} U_i(r_{1i} + r_{2i} + ... + r_{Ki}) \\
\text{subject to} \quad & \sum_{i=1}^{M} r_{1i} \le R_1, \sum_{i=1}^{M} r_{2i} \le R_2, ... \\
& ... , \sum_{i=1}^{M} r_{Ki} \le R_K, \\
& r_{li} \ge 0, \quad l = 1, 2, ..., K, \quad i = 1, 2, ..., M
\end{aligned} \quad (4)
$$

where R_l is the total available rate at the lth carrier eNodeB.

We prove in Section III that the solution of the optimization problem (4) is the global optimal solution.

III. THE GLOBAL OPTIMAL SOLUTION

In the optimization problem (4), since the objective function $\arg\max_{\mathbf{r}} \prod_{i=1}^{M} U_i(r_{1i} + r_{2i} + ... + r_{Ki})$ is equivalent to $\arg\max_{\mathbf{r}} \sum_{i=1}^{M} \log(U_i(r_{1i} + r_{2i} + ... + r_{Ki}))$, then optimization problem (4) can be written as:

$$
\begin{aligned}
\max_{\mathbf{r}} \quad & \sum_{i=1}^{M} \log\Big(U_i(r_{1i} + r_{2i} + ... + r_{Ki}) \Big) \\
\text{subject to} \quad & \sum_{i=1}^{M} r_{1i} \le R_1, \sum_{i=1}^{M} r_{2i} \le R_2, ... \\
& ... , \sum_{i=1}^{M} r_{Ki} \le R_K, \\
& r_{li} \ge 0, \quad l = 1, 2, ..., K, \quad i = 1, 2, ..., M.
\end{aligned} \quad (5)
$$

Lemma III.1. *The utility functions $\log(U_i(r_{1i} + ... + r_{Ki}))$ in the optimization problem (5) are strictly concave functions.*

Proof: In Section II, we assume that all the utility functions of the UEs are strictly concave or sigmoidal-like functions.

In the strictly concave utility function case, recall the utility function properties in Section II, the utility function is positive $U_i(r_{1i} + ... + r_{Ki}) > 0$, increasing and twice differentiable with respect to r_{li}. Then, it follows that $\frac{\partial U_i(r_{1i}+...+r_{Ki})}{\partial r_{li}} > 0$ and $\frac{\partial^2 U_i(r_{1i}+...+r_{Ki})}{\partial r_{li}^2} < 0$. It follows that, the utility function $\log(U_i(r_{1i} + r_{2i} + ... + r_{Ki}))$ in the optimization problem (5) have

$$\frac{\partial \log(U_i(r_{1i} + ... + r_{Ki}))}{\partial r_{li}} = \frac{\frac{\partial U_i}{\partial r_{li}}}{U_i} > 0 \tag{6}$$

and

$$\frac{\partial^2 \log(U_i(r_{1i} + ... + r_{Ki}))}{\partial r_{li}^2} = \frac{\frac{\partial^2 U_i}{\partial r_{li}^2}U_i - (\frac{\partial U_i}{\partial r_{li}})^2}{U_i^2} < 0. \tag{7}$$

Therefore, the strictly concave utility function $U_i(r_{1i} + r_{2i} + ... + r_{Ki})$ natural logarithm $\log(U_i(r_{1i} + r_{2i} + ... + r_{Ki}))$ is also strictly concave. It follows that the natural logarithm of the logarithmic utility function in equation (2) is strictly concave.

In the sigmoidal-like utility function case, the utility function of the normalized sigmoidal-like function is given by equation (1) as $U_i(r_{1i} + r_{2i} + ... + r_{Ki}) = c_i\left(\frac{1}{1+e^{-a_i(\sum_{l=1}^{K} r_{li}-b_i)}} - d_i\right)$. For $0 < \sum_{l=1}^{K} r_{li} < \sum_{l=1}^{K} R_l$, we have

$$0 < c_i\left(\frac{1}{1 + e^{-a_i(\sum_{l=1}^{K} r_{li}-b_i)}} - d_i\right) < 1$$

$$d_i < \frac{1}{1 + e^{-a_i(\sum_{l=1}^{K} r_{li}-b_i)}} < \frac{1 + c_i d_i}{c_i}$$

$$\frac{1}{d_i} > 1 + e^{-a_i(\sum_{l=1}^{K} r_{li}-b_i)} > \frac{c_i}{1 + c_i d_i}$$

$$0 < 1 - d_i(1 + e^{-a_i(\sum_{l=1}^{K} r_{li}-b_i)}) < \frac{1}{1 + c_i d_i}$$

It follows that for $0 < \sum_{l=1}^{K} r_{li} < \sum_{l=1}^{K} R_l$, we have the first and second derivative as

$$\frac{\partial}{\partial r_{li}} \log U_i(r_{1i} + ... + r_{Ki}) = \frac{a_i d_i e^{-a_i(\sum_{l=1}^{K} r_{li}-b_i)}}{1 - d_i(1 + e^{-a_i(\sum_{l=1}^{K} r_{li}-b_i)})}$$
$$+ \frac{a_i e^{-a_i(\sum_{l=1}^{K} r_{li}-b_i)}}{(1 + e^{-a_i(\sum_{l=1}^{K} r_{li}-b_i)})} > 0$$

$$\frac{\partial^2}{\partial r_{li}^2} \log U_i(r_{1i} + ... + r_{Ki}) = \frac{-a_i^2 d_i e^{-a_i(\sum_{l=1}^{K} r_{li}-b_i)}}{c_i\left(1 - d_i(1 + e^{-a(\sum_{l=1}^{K} r_{li}-b_i)})\right)^2}$$
$$+ \frac{-a_i^2 e^{-a_i(\sum_{l=1}^{K} r_{li}-b_i)}}{(1 + e^{-a_i(\sum_{l=1}^{K} r_{li}-b_i)})^2} < 0$$

Therefore, the sigmoidal-like utility function $U_i(r_{1i}+...+r_{Ki})$ natural logarithm $\log(U_i(r_{1i} + ... + r_{Ki}))$ is strictly concave function. Therefore, all the utility functions in our model have strictly concave natural logarithm. ∎

Theorem III.2. *The optimization problem (4) is a convex optimization problem and there exists a unique tractable global optimal solution.*

Proof: It follows from Lemma III.1 that for all UEs utility functions are strictly concave. Therefore, the optimization problem (5) is a convex optimization problem [39]. The optimization problem (5) is equivalent to optimization problem (4), therefore it is a convex optimization problem. For a convex optimization problem, there exists a unique tractable global optimal solution [39]. ∎

IV. THE DUAL PROBLEM

The key to a distributed and decentralized optimal solution of the primal problem in (5) is to convert it to the dual problem similar to [12], [13] and [40]. The optimization problem (5) can be divided into two simpler problems by using the dual problem. We define the Lagrangian

$$\begin{aligned}
L(\mathbf{r}, \mathbf{p}) &= \sum_{i=1}^{M} \log\left(U_i(r_{1i} + r_{2i} + ... + r_{Ki})\right) \\
&- p_1(\sum_{i=1}^{M} r_{1i} + z_1 - R_1) - ... \\
&- p_K(\sum_{i=1}^{M} r_{Ki} + z_K - R_K) \\
&= \sum_{i=1}^{M} \left(\log(U_i(r_{1i} + r_{2i} + ... + r_{Ki})) - \sum_{l=1}^{K} p_l r_{li}\right) \\
&+ \sum_{l=1}^{K} p_l(R_l - z_l) \\
&= \sum_{i=1}^{M} L_i(\mathbf{r}_i, \mathbf{p}) + \sum_{l=1}^{K} p_l(R_l - z_l)
\end{aligned} \tag{8}$$

where $z_l \geq 0$ is the lth slack variable and p_l is Lagrange multiplier or the shadow price of the lth carrier eNodeB (i.e. the total price per unit rate for all the users in the coverage area of the lth carrier eNodeB) and $\mathbf{p} = \{p_1, p_2, ..., p_K\}$. Therefore, the ith UE bid for rate from the lth carrier eNodeB can be written as $w_{li} = p_l r_{li}$ and we have $\sum_{i=1}^{M} w_{li} = p_l \sum_{i=1}^{M} r_{li}$. The first term in equation (8) is separable in $\mathbf{r}_i$. So we have $\max_{\mathbf{r}} \sum_{i=1}^{M} (\log(U_i(r_{1i} + r_{2i} + ... + r_{Ki})) - \sum_{l=1}^{K} p_l r_{li}) = \sum_{i=1}^{M} \max_{\mathbf{r}_i} (\log(U_i(r_{1i} + r_{2i} + ... + r_{Ki})) - \sum_{l=1}^{K} p_l r_{li})$. The dual problem objective function can be written as

$$\begin{aligned}
D(\mathbf{p}) &= \max_{\mathbf{r}} L(\mathbf{r}, \mathbf{p}) \\
&= \sum_{i=1}^{M} \max_{\mathbf{r}_i}(L_i(\mathbf{r}_i, \mathbf{p})) + \sum_{l=1}^{K} p_l(R_l - z_l)
\end{aligned} \tag{9}$$

The dual problem is given by

$$\begin{aligned}
\min_{\mathbf{p}} \quad &D(\mathbf{p}) \\
\text{subject to} \quad &p_l \geq 0, \quad l = 1, 2, ..., K.
\end{aligned} \tag{10}$$

So we have

$$\frac{\partial D(\mathbf{p})}{\partial p_l} = R_l - \sum_{i=1}^{M} r_{li} - z_l = 0 \tag{11}$$

substituting by $\sum_{i=1}^{M} w_{li} = p_l \sum_{i=1}^{M} r_{li}$ we have

$$p_l = \frac{\sum_{i=1}^{M} w_{li}}{R_l - z_l}. \tag{12}$$

Now, we divide the primal problem (5) into two simpler optimization problems in the UEs and the eNodeBs. The ith UE optimization problem is given by:

$$\max_{r_i} \quad \log(U_i(r_{1i} + r_{2i} + ... + r_{Ki})) - \sum_{l=1}^{K} p_l r_{li}$$
$$\text{subject to} \quad p_l \geq 0 \tag{13}$$
$$r_{li} \geq 0, \quad i = 1, 2, ..., M, l = 1, 2, ..., K.$$

The second problem is the lth eNodeB optimization problem for rate proportional fairness that is given by:

$$\min_{p_l} \quad D(\mathbf{p})$$
$$\text{subject to} \quad p_l \geq 0. \tag{14}$$

The minimization of shadow price p_l is achieved by the minimization of the slack variable $z_l \geq 0$ from equation (12). Therefore, the maximum utility percentage of the lth eNodeB rate R_l is achieved by setting the slack variable $z_l = 0$. In this case, we replace the inequality in primal problem (5) constraints by equality constraints and so we have $\sum_{i=1}^{M} w_{li} = p_l R_l$. Therefore, we have $p_l = \frac{\sum_{i=1}^{M} w_{li}}{R_l}$ where $w_{li} = p_l r_{li}$ is transmitted by the ith UE to l^{th} eNodeB. The utility proportional fairness in the objective function of the optimization problem (4) is guaranteed in the solution of the optimization problems (13) and (14).

V. DISTRIBUTED OPTIMIZATION ALGORITHM

The distributed resource allocation algorithm, in [1], for optimization problems (13) and (14) is a modified version of the distributed algorithms in [12], [20], [21], [13] and [40], which is an iterative solution for allocating the network resources for a single carrier. The algorithm in [1] allocates resources from multiple carriers simultaneously with utility proportional fairness policy. The algorithm is divided into the ith UE algorithm as shown in Algorithm 1 [1] and the lth eNodeB carrier algorithm as shown in Algorithm 2 [1]. In Algorithm 1 and 2 [1], the ith UE starts with an initial bid $w_{li}(1)$ which is transmitted to the lth carrier eNodeB. The lth eNodeB calculates the difference between the received bid $w_{li}(n)$ and the previously received bid $w_{li}(n-1)$ and exits if it is less than a pre-specified threshold δ. We set $w_{li}(0) = 0$. If the value is greater than the threshold, the lth eNodeB calculates the shadow price $p_l(n) = \frac{\sum_{i=1}^{M} w_{li}(n)}{R_l}$ and sends that value to all UEs in its coverage area. The ith UE receives the shadow prices p_l from all in range carriers eNodeBs and compares them to find the first minimum shadow price $p_{\min}^1(n)$ and the corresponding carrier index $l_1 \in L$ where $L = \{1, 2, ..., K\}$. The ith UE solves for the l_1 carrier rate $r_{l_1 i}(n)$ that maximizes
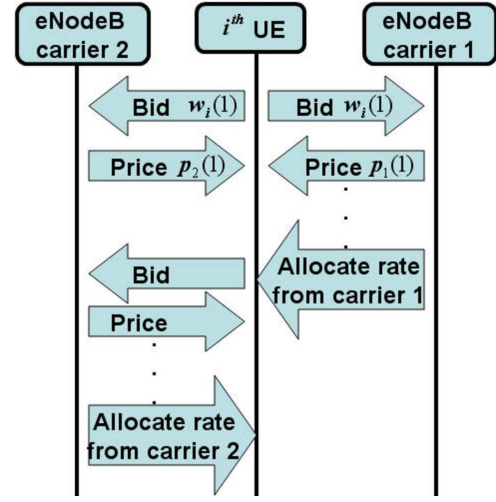

Fig. 1. Flow Diagram with the assumption that the shadow price from the first carrier eNodeB p_1 is less before the n_1th iteration so rate r_{1i} of the ith user is allocated. After the n_1th iteration, the shadow price from the second carrier eNodeB p_2 is less so rate r_{2i} is allocated.

$\log U_i(r_{1i} + ... + r_{Ki}) - \sum_{l=1}^{K} p_l(n) r_{li}$ with respect to $r_{l_1 i}$. The rate $r_i^1(n) = r_{l_1 i}(n)$ is used to calculate the new bid $w_{l_1 i}(n) = p_{\min}^1(n) r_i^1(n)$. The ith UE sends the value of its new bid $w_{l_1 i}(n)$ to the l_1 carrier eNodeB. Then, the ith UE selects the second minimum shadow price $p_{\min}^2(n)$ and the corresponding carrier index $l_2 \in L$. The ith UE solves for the l_2 carrier rate $r_{l_2 i}(n)$ that maximizes $\log U_i(r_{1i} + ... + r_{Ki}) - \sum_{l=1}^{K} p_l(n) r_{li}$ with respect to $r_{l_2 i}$. The rate $r_{l_2 i}(n)$ subtracted by the rate from l_1 carrier $r_i^2(n) = r_{l_2 i}(n) - r_i^1(n)$ is used to calculate the new bid $w_{l_2 i}(n) = p_{\min}^2(n) r_i^2(n)$ which is sent to l_2 carrier eNodeB. In general, the ith UE selects the mth minimum shadow price $p_{\min}^m(n)$ with carrier index $l_m \in L$ and solves for the l_m carrier rate $r_{l_m i}(n)$ that maximizes $\log U_i(r_{1i} + ... + r_{Ki}) - \sum_{l=1}^{K} p_l(n) r_{li}$ with respect to $r_{l_m i}$. The rate $r_{l_m i}(n)$ subtracted by $l_1, l_2, ..., l_{m-1}$ carriers rates $r_i^m(n) = r_{l_m i}(n) - (r_i^1(n) + r_i^2(n) + ... + r_i^{m-1}(n))$ is used to calculate the new bid $w_{l_m i}(n) = p_{\min}^m(n) r_i^m(n)$ which is sent to l_m carrier eNodeB. This process is repeated until $|w_{li}(n) - w_{li}(n-1)|$ is less than the threshold δ for all l carriers.

The distributed algorithm in [1] is set to avoid the situation of allocating zero rate to any user (i.e. no user is dropped). This is inherited from the utility proportional fairness policy in the optimization problem, similar to [12], [20] and [21]. In addition, the UE chooses from the nearby carriers eNodeBs the one with the lowest shadow price and starts requesting bandwidth from that carrier eNodeB. If the allocated rate is not enough or the price of the resources increases due to high demand on that carrier eNodeB resources from other UEs, the UE switches to another nearby eNodeB carrier with a lower resource price to be allocated the rest of the required resources. This is done iteratively until an equilibrium between demand and supply of resources is achieved and the optimal rates are allocated in the LTE mobile network. Figure 1 shows a block diagram that represents the distributed RA algorithm.

VI. Convergence Analysis

In this section, we present the convergence analysis of Algorithm 1 and 2 in [1] for different values of carriers eNodeBs rates R_l. This analysis is equivalent to low and high-traffic hours analysis in cellular systems (e.g. change in the number of active users M and their traffic in the cellular system [20]).

A. Drawback in Algorithm 1 and 2 in [1]

Lemma VI.1. *For sigmoidal-like utility function $U_i(r_{1i}+r_{2i}+...+r_{Ki})$, the slope curvature function $\frac{\partial \log U_i(r_{1i}+r_{2i}+...+r_{Ki})}{\partial r_{li}}$ has an inflection point at $\sum_{l=1}^{K} r_{li} = r_i^s \approx b_i$ and is convex for $\sum_{l=1}^{K} r_{li} > r_i^s$.*

Proof: For the sigmoidal-like function $U_i(r_{1i}+r_{2i}+...+r_{Ki}) = c_i\left(\frac{1}{1+e^{-a_i(\sum_{l=1}^{K} r_{li}-b_i)}} - d_i\right)$, let $S_i(r_{li}) = \frac{\partial \log U_i(r_{1i}+r_{2i}+...+r_{Ki})}{\partial r_{li}}$ be the slope curvature function. Then, we have that

$$\frac{\partial S_i}{\partial r_{li}} = \frac{-a_i^2 d_i e^{-a_i(\sum_{l=1}^{K} r_{li}-b_i)}}{c_i\left(1 - d_i(1+e^{-a_i(\sum_{l=1}^{K} r_{li}-b_i)})\right)^2}$$
$$- \frac{a_i^2 e^{-a_i(\sum_{l=1}^{K} r_{li}-b_i)}}{\left(1+e^{-a_i(\sum_{l=1}^{K} r_{li}-b_i)}\right)^2}$$

and

$$\frac{\partial^2 S_i}{\partial r_{li}^2} = \frac{a_i^3 d_i e^{-a_i(\sum_{l=1}^{K} r_{li}-b_i)}\left(1 - d_i(1 - e^{-a_i(\sum_{l=1}^{K} r_{li}-b_i)})\right)}{c_i\left(1 - d_i(1+e^{-a_i(\sum_{l=1}^{K} r_{li}-b_i)})\right)^3}$$
$$+ \frac{a_i^3 e^{-a_i(\sum_{l=1}^{K} r_{li}-b_i)}\left(1 - e^{-a_i(\sum_{l=1}^{K} r_{li}-b_i)}\right)}{\left(1+e^{-a_i(\sum_{l=1}^{K} r_{li}-b_i)}\right)^3}. \tag{15}$$

We analyze the curvature of the slope of the natural logarithm of sigmoidal-like utility function. For the first derivative, we have $\frac{\partial S_i}{\partial r_{li}} < 0 \ \forall r_{li}$. The first term S_i^1 of $\frac{\partial^2 S_i}{\partial r_{li}^2}$ in equation (15) can be written as

$$S_i^1 = \frac{a_i^3 e^{a_i b_i}\left(e^{a_i b_i} + e^{-a_i(\sum_{l=1}^{K} r_{li}-b_i)}\right)}{(e^{a_i b_i} - e^{-a_i(\sum_{l=1}^{K} r_{li}-b_i)})^3} \tag{16}$$

and we have the following properties:

$$\begin{cases} \lim_{\sum_{l=1}^{K} r_{li}\to 0} S_i^1 = \infty, \\ \lim_{\sum_{l=1}^{K} r_{li}\to b_i} S_i^1 = 0 \text{ for } b_i \gg \frac{1}{a_i}. \end{cases} \tag{17}$$

For second term S_i^2 of $\frac{\partial^2 S_i}{\partial r_i^2}$ in equation (15), we have the following properties:

$$\begin{cases} S_i^2(r_{li} = b_i - \sum_{j\neq l} r_{ji}) = 0, \\ S_i^2(r_{li} > b_i - \sum_{j\neq l} r_{ji}) > 0, \\ S_i^2(r_{li} < b_i - \sum_{j\neq l} r_{ji}) < 0. \end{cases} \tag{18}$$

From equation (17) and (18), S_i has an inflection point at $\sum_{l=1}^{K} r_{li} = r_i^s \approx b_i$. In addition, we have the curvature of S_i changes from a convex function close to origin to a concave function before the inflection point $\sum_{l=1}^{K} r_{li} = r_i^s$ then to a convex function after the inflection point. ∎

Our rate allocation approach guarantees non-zero rate allocation for all active users in the coverage area of a specific carrier eNodeB. We define the set $\mathcal{M}^l := \{i : r_{li} \neq 0\}$ to be the set of active users covered by the lth eNodeB. Then, we have the following Corollary.

Corollary VI.2. *If $\sum_{i\in\mathcal{M}^l} r_i^{inf} \ll R_l \ \forall \ l \in L$ then Algorithm 1 and 2 in [1] converge to the global optimal rates which correspond to the steady state shadow price $p_{ss} < \frac{a_{i_{\max}} d_{i_{\max}}}{1-d_{i_{\max}}} + \frac{a_{i_{\max}}}{2}$ where $i_{\max} = \arg\max_{i\in\mathcal{M}^l} b_i$.*

Proof: For the sigmoidal-like function $U_i(r_{1i} + r_{2i} + ... + r_{Ki}) = c_i\left(\frac{1}{1+e^{-a_i(\sum_{l=1}^{K} r_{li}-b_i)}} - d_i\right)$, the optimal solution is achieved by solving the optimization problem (5). In Algorithm 1 [1], an important step to reach to the optimal solution is to solve the optimization problem $r_{li}(n) = \arg\max_{r_{li}}\left(\log U_i(r_{1i} + r_{2i} + ... + r_{Ki}) - p_l(n)r_{li}\right)$ for every UE in the lth eNodeB coverage area. The solution of this problem can be written, using Lagrange multipliers method, in the form

$$\frac{\partial \log U_i(r_{1i} + r_{2i} + ... + r_{Ki})}{\partial r_{li}} - p_l = S_i(r_{li}) - p_l = 0. \tag{19}$$

From equation (17) and (18) in Lemma VI.1, we have the curvature of $S_i(r_{li})$ is convex for $\sum_{l=1}^{K} r_{li} > r_i^s \approx b_i$. The algorithm in [1] is guaranteed to converge to the global optimal solution when the slope $S_i(r_{li})$ of all the utility functions natural logarithm $\log U_i(r_{1i}+r_{2i}+...+r_{Ki})$ are in the convex region of the functions, similar to analysis of logarithmic functions in [13] and [40]. Therefore, the natural logarithm of sigmoidal-like functions $\log U_i(r_{1i}+r_{2i}+...+r_{Ki})$ converge to the global optimal solution for $\sum_{l=1}^{K} r_{li} > r_i^s \approx b_i$. The inflection point of sigmoidal-like function $U_i(r_{1i}+r_{2i}+ ... + r_{Ki})$ is at $r_i^{inf} = b_i$. For $\sum_{i\in\mathcal{M}^l} r_i^{inf} \ll R_l$, the algorithm in [1] allocates rates $\sum_{l=1}^{K} r_{li} > b_i$ for all users. Since $S_i(r_{li})$ is convex for $\sum_{l=1}^{K} r_{li} > r_i^s \approx b_i$ then the optimal solution can be achieved by Algorithm 1 and 2 in [1]. We have from equation (19) and as $S_i(r_{li})$ is convex for $\sum_{l=1}^{K} r_{li} > r_i^s \approx b_i$, that $p_{ss} < S_i(\sum_{l=1}^{K} r_{li} = \max_{i\in\mathcal{M}^l} b_i)$ where $S_i(\sum_{l=1}^{K} r_{li} = \max_{i\in\mathcal{M}^l} b_i) = \frac{a_{i_{\max}} d_{i_{\max}}}{1-d_{i_{\max}}} + \frac{a_{i_{\max}}}{2}$ and $i_{\max} = \arg\max_{i\in\mathcal{M}^l} b_i$. ∎

We define the set $\mathcal{M}^{\mathcal{L}} := \{i : r_{li} \neq 0 \ \forall l \in \mathcal{L}, r_{li} = 0 \ \forall l \notin \mathcal{L}\}$ to be the set of active users covered exclusively by the set of carriers eNodeBs $\mathcal{L} \subseteq L$. Then, we have the following Corollary.

Corollary VI.3. *For $\sum_{i\in\mathcal{M}^{\mathcal{L}}} r_i^{inf} > \sum_{l\in\mathcal{L}} R_l$ and the global optimal shadow price $p_{ss} \approx \frac{a_i d_i e^{\frac{a_i b_i}{2}}}{1-d_i(1+e^{\frac{a_i b_i}{2}})} + \frac{a_i e^{\frac{a_i b_i}{2}}}{(1+e^{\frac{a_i b_i}{2}})}$ where $i \in \mathcal{M}^{\mathcal{L}}$, then the solution given by Algorithm 1 and 2 in [1] fluctuates about the global optimal rates.*

Proof: For the sigmoidal-like function $U_i(r_{1i} + r_{2i} + ... + r_{Ki}) = c_i\left(\frac{1}{1+e^{-a_i(\sum_{l=1}^{K} r_{li}-b_i)}} - d_i\right)$, it follows from lemma VI.1 that for $\sum_{i\in\mathcal{M}^{\mathcal{L}}} r_i^{inf} > \sum_{l\in\mathcal{L}} R_l \ \exists \ i \in \mathcal{M}^{\mathcal{L}}$ such that the optimal rates $\sum_{l=1}^{K} r_{li}^{opt} < b_i$. Therefore, if $p_{ss} \approx \frac{a_i d_i e^{\frac{a_i b_i}{2}}}{1-d_i(1+e^{\frac{a_i b_i}{2}})} + \frac{a_i e^{\frac{a_i b_i}{2}}}{(1+e^{\frac{a_i b_i}{2}})}$ is the optimal shadow price

Algorithm VI.1 The ith UE Algorithm
___
Send initial bid $w_{li}(1)$ to l^{th} carrier eNodeB (where $l \in L = \{1, 2, ..., K\}$)
loop
  Receive shadow prices $p_{l \in L}(n)$ from all in range carriers eNodeBs
  if STOP from all in range carriers eNodeBs **then**
    Calculate allocated rates $r_{li}^{\text{opt}} = \frac{w_{li}(n)}{p_l(n)}$
    STOP
  else
    Set $p_{\min}^0 = \{\}$ and $r_i^0 = 0$
    for $m = 1 \rightarrow K$ **do**
      $p_{\min}^m(n) = \min(\mathbf{p} \setminus \{p_{\min}^0, p_{\min}^1, ..., p_{\min}^{m-1}\})$
      $l_m = \{l \in L : p_l = \min(\mathbf{p} \setminus \{p_{\min}^0, p_{\min}^1, ..., p_{\min}^{m-1}\})\}$ {l_m is the index of the corresponding carrier}
      Solve $r_{l_m i}(n) = \arg \max_{r_{l_m i}} \Big(\log U_i(r_{1i} + ... + r_{Ki}) - \sum_{l=1}^K p_l(n) r_{li} \Big)$ for the l_m carrier eNodeB
      $r_i^m(n) = r_{l_m i}(n) - \sum_{j=0}^{m-1} r_i^j(n)$
      if $r_i^m(n) < 0$ **then**
        Set $r_i^m(n) = 0$
      end if
      Calculate new bid $w_{l_m i}(n) = p_{\min}^m(n) r_i^m(n)$
      if $|w_{l_m i}(n) - w_{l_m i}(n-1)| > \Delta w(n)$ **then**
        $w_{l_m i}(n) = w_i(n-1) + \text{sign}(w_{l_m i}(n) - w_{l_m i}(n-1)) \Delta w(n)$ {$\Delta w = h_1 e^{-\frac{n}{h_2}}$ or $\Delta w = \frac{h_3}{n}$}
      end if
      Send new bid $w_{l_m i}(n)$ to l_m carrier eNodeB
    end for
  end if
end loop

Algorithm VI.2 The lth eNodeB Algorithm
___
loop
  Receive bids $w_{li}(n)$ from UEs {Let $w_{li}(0) = 0 \; \forall i$}
  if $|w_{li}(n) - w_{li}(n-1)| < \delta \; \forall i$ **then**
    Allocate rates, $r_{li}^{\text{opt}} = \frac{w_{li}(n)}{p_l(n)}$ to i^{th} UE
    STOP
  else
    Calculate $p_l(n) = \frac{\sum_{i=1}^M w_{li}(n)}{R_l}$
    Send new shadow price $p_l(n)$ to all UEs
  end if
end loop

$\sum_{l \in \mathcal{L}} R_l$, robust algorithm avoids the fluctuation in the non-convergent region discussed in the previous section. This is achieved by adding a convergence measure $\Delta w(n)$ that senses the fluctuation in the bids w_{li}. In case of fluctuation, it decreases the step size between the current and the previous bid $w_{li}(n) - w_{li}(n-1)$ for every user i using *fluctuation decay function*. The fluctuation decay function could be in the following forms:

- *Exponential function*: It takes the form $\Delta w(n) = h_1 e^{-\frac{n}{h_2}}$.
- *Rational function*: It takes the form $\Delta w(n) = \frac{h_3}{n}$.

where h_1, h_2, h_3 can be adjusted to change the rate of decay of the bids w_{li}.

Remark VI.5. *The fluctuation decay function can be included in the UE or the eNodeB Algorithm.*

In our model, we add the decay part to the UE Algorithm as shown in Algorithm VI.1.

VII. SIMULATION RESULTS

Algorithm VI.1 and VI.2 were applied to various logarithmic and sigmoidal-like utility functions with different parameters in MATLAB. The simulation results showed convergence to the global optimal rates. In this section, we present the simulation results for two carriers in a heterogeneous network (HetNet) that consists of one macro cell, one small cell and 12 active UEs as shown in Figure 2. The UEs are divided into two groups. The 1st group of UEs (index $i = \{1, 2, 3, 4, 5, 6\}$) is located in the macro cell under the coverage area of both the 1st carrier (C1) and the 2nd carrier (C2) eNodeBs. We use three normalized sigmoidal-like functions that are expressed by equation (1) with different parameters. The used parameters are $a = 5$, $b = 10$ corresponding to a sigmoidal-like function that is an approximation to a step function at rate $r = 10$ (e.g. VoIP) and is the utility of UEs with indexes $i = \{1, 7\}$, $a = 3$, $b = 20$ corresponding to a sigmoidal-like function that is an approximation of an adaptive real-time application with inflection point at rate $r = 20$ (e.g. standard definition video streaming) and is the utility of UEs with indexes $i = \{2, 8\}$, and $a = 1$, $b = 30$ corresponding to a sigmoidal-like function that is also an approximation of an adaptive real-time application with inflection point at rate $r = 30$ (e.g. high definition video streaming) and is the utility of UEs with indexes $i = \{3, 9\}$, as shown in Figure 3. We
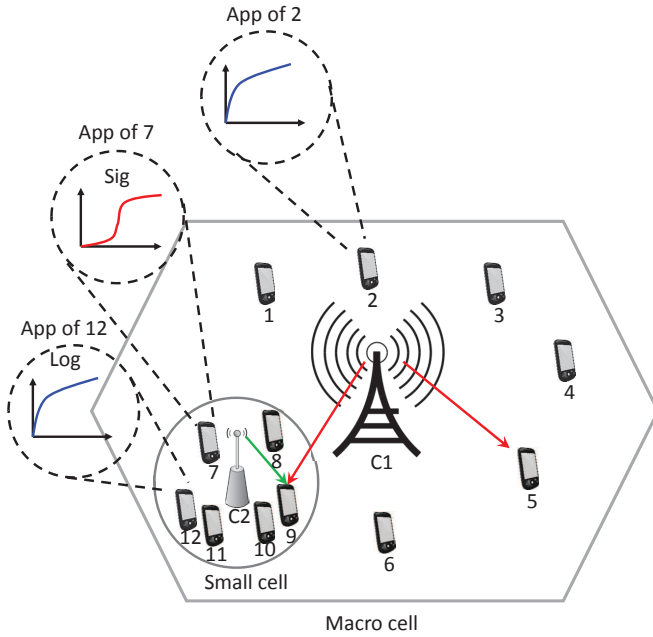
for optimization problem (5). Then, a small change in the shadow price $p_l(n)$ in the nth iteration can lead the rate $r_{li}(n)$ (root of $S_i(r_{li}) - p_l(n) = 0$) to fluctuate between the concave and convex curvature of the slope curve $S_i(r_{li})$ for the ith user. Therefore, it causes fluctuation in the bid $w_{li}(n)$ sent to the eNodeB and fluctuation in the shadow price $p_l(n)$ set by eNodeB. Therefore, the iterative solution of Algorithm 1 and 2 in [1] fluctuates about the global optimal rates $\sum_{l=1}^K r_{li}^{\text{opt}}$. ∎

Theorem VI.4. *Algorithm 1 and 2 in [1] does not converge to the global optimal rates for all values of R_l.*

Proof: It follows from Corollary VI.2 and VI.3 that Algorithm 1 and 2 in [1] does not converge to the global optimal rates for all values of R_l. ∎

B. Solution using Algorithm VI.1 and VI.2

For a robust algorithm, we add a fluctuation decay function to the algorithm presented in [1] as shown in Algorithm VI.1. Our robust algorithm ensures convergence for all values of the carriers eNodeBs maximum rate R_l for all l. Algorithm VI.1 and VI.2 allocated rates coincide with Algorithm 1 and 2 in [1] for $\sum_{i \in \mathcal{M}^l} r_i^{\text{inf}} \ll R_l \; \forall \; l \in L$. For $\sum_{i \in \mathcal{M}^{\mathcal{L}}} r_i^{\text{inf}} >$

Fig. 2. System model with two groups of users. The 1st group with UE indexes $i = \{1, 2, 3, 4, 5, 6\}$, 2nd group with UE indexes $i = \{7, 8, 9, 10, 11, 12\}$.
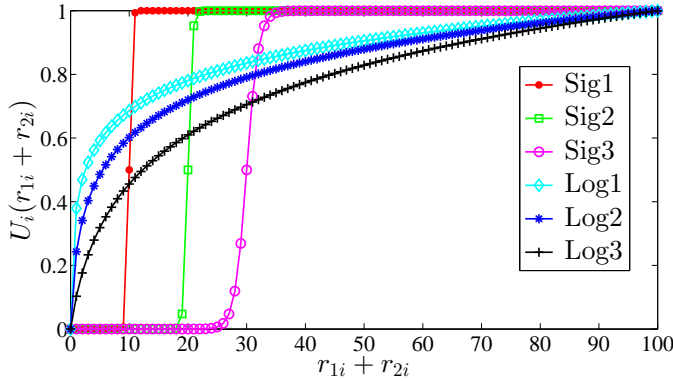

Fig. 4. The sigmoidal-like utility $U_i(r_{1i}+r_{2i}) = c_i(\frac{1}{1+e^{-a_i(r_{1i}+r_{2i}-b_i)}} - d_i)$ of the ith user, where r_{1i} is the rate allocated by 1st carrier eNodeB and r_{2i} is the rate allocated by 2nd carrier eNodeB.

Fig. 3. The users utility functions $U_i(r_{1i} + r_{2i})$ used in the simulation (three sigmoidal-like functions and three logarithmic functions).

TABLE I
USERS AND THEIR APPLICATIONS UTILITIES

Applications Utilities Parameters		Users Indexes
Sig1	Sig $a = 5$, $b = 10$	$i = \{1, 7\}$
Sig2	Sig $a = 3$, $b = 20$	$i = \{2, 8\}$
Sig3	Sig $a = 1$, $b = 30$	$i = \{3, 9\}$
Log1	Log $k = 15$, $r_{max} = 100$	$i = \{4, 10\}$
Log2	Log $k = 3$, $r_{max} = 100$	$i = \{5, 11\}$
Log3	Log $k = 0.5$, $r_{max} = 100$	$i = \{6, 12\}$

use three logarithmic functions that are expressed by equation (2) with $r_{max} = 100$ and different k_i parameters which are approximations for delay-tolerant applications (e.g. FTP). We use $k = 15$ for UEs with indexes $i = \{4, 10\}$, $k = 3$ for UEs with indexes $i = \{5, 11\}$, and $k = 0.5$ for UEs with indexes $i = \{6, 12\}$, as shown in Figure 3. A summary is shown in table I. A three dimensional view of the sigmoidal-like utility function $U_i(r_{1i} + r_{2i})$ is show in Figure 4.

A. Allocated Rates for $30 \leq R_1 \leq 200$ and $R_2 = 70$

In the following simulations, we set $\delta = 10^{-3}$, the 1st carrier eNodeB rate R_1 takes values between 30 and 200 with step of 10, and the 2nd carrier eNodeB rate is fixed at $R_2 = 70$. In Figure 5, we show the final allocated optimal rates $r_i = r_{1i} + r_{2i}$ of different users with different 1st carrier eNodeB total rate R_1 and observe how the proposed rate allocation algorithm converges when the eNodeBs available resources are
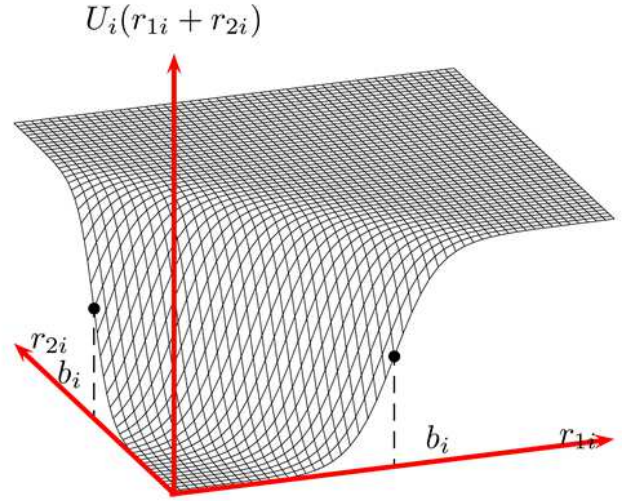
abundant or scarce. In Figure 5(a), we show the rates allocated to the 1st group of UEs by only C1 eNodeB since C2 eNodeB is not within these users range, we observe the increase in the rate allocated to these users with the increase in R_1. Figure 5(b) shows the final allocated rates to the 2nd group of UEs by both C1 and C2 eNodeBs. Since these users located under the coverage area of both the macro cell and the small cell, they are allocated rates jointly using the proposed RA with joint CA approach. Figure 5(a) and 5(b) show that by using the RA with joint CA algorithm, no user is allocated zero rate (i.e. no user is dropped). However, the majority of the eNodeBs resources are allocated to the UEs running adaptive real-time applications until they reach their inflection rates the eNodeBs then allocate more resources to the UEs with delay-tolerant applications, as real-time application users bid higher than delay-tolerant application users by using the utility proportional fairness policy.

In Figure 6, we show the rates allocated to the 2nd group users, located under the coverage area of both the macro cell and small cell eNodeBs, by each of the two carriers' eNodeBs with the increase in the 1st carrier eNodeB resources. In Figure 6(a) and 6(b), when the resources available at C2 eNodeB (i.e. R_2) is more than that at C1 eNodeB, we observe that most of the 2nd group rates are allocated by C2 eNodeB. However, the
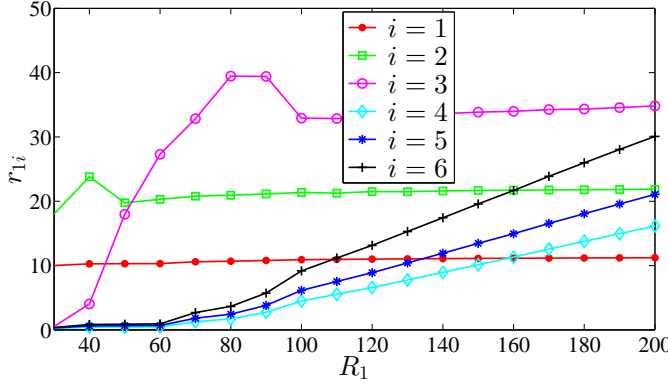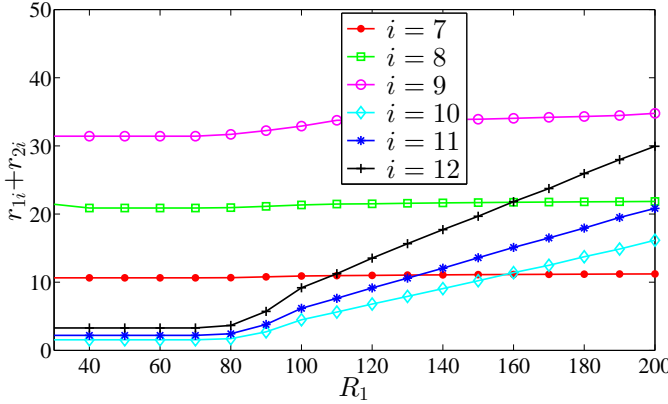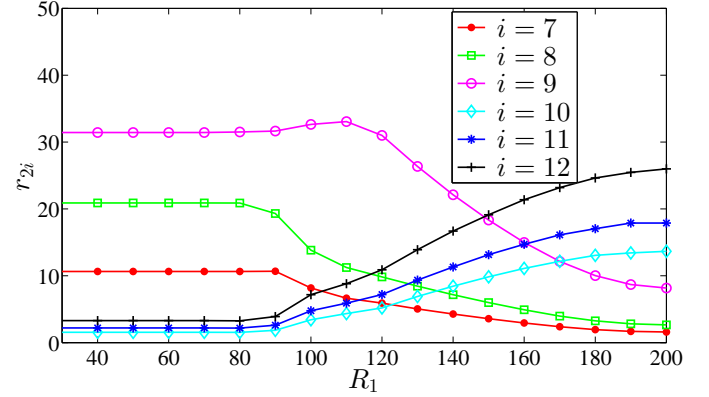
(a) The rates allocated r_{1i} from the 1st carrier eNodeB (i.e. the macro cell eNodeB) to users of the 1st group (i.e. $i = 1, 2, 3, 4, 5, 6$).
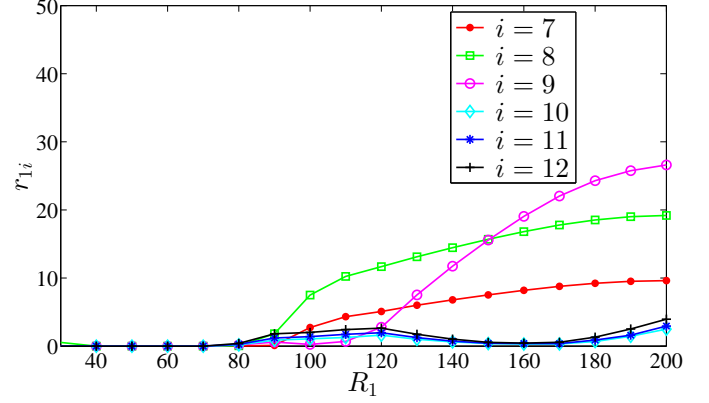
(a) The allocated rates r_{1i} from the 1st carrier eNodeB to the 2nd group of users.

(b) The rates $r_{1i} + r_{2i}$ allocated from 1st and 2nd carriers eNodeBs (i.e. the macro cell and the small cell eNodeBs) to users of the 2nd group (i.e. $i = 7, 8, 9, 10, 11, 12$).

Fig. 5. The allocated rates $\sum_{l=1}^{K} r_{li}$ of the two groups of users verses 1st carrier rate $30 < R_1 < 200$ with 2nd carrier rate fixed at $R_2 = 70$.

(b) The allocated rates r_{2i} from the 2nd carrier eNodeB to the 2nd group of users.

Fig. 6. The allocated rates from C1 and C2 eNodeBs to the 2nd group of users with 1st carrier eNodeB rate $30 < R_1 < 200$ and 2nd carrier eNodeB rate fixed at $R_2 = 70$.

delay tolerant applications are not allocated much resources since most of R_2 is allocated to the real-time applications. With the increase in C1 eNodeB resources R_1, we observe a gradual increase in the 2nd group rates allocated to real-time applications from C1 eNodeB and a gradual decrease from C2 eNodeB resources allocated to real-time-applications. This shift in the resource allocation increases the available resources in C2 eNodeB to be allocated to 2nd group delay tolerant applications by C2 eNodeB.

B. Pricing Analysis and Comparison for $30 \leq R_1 \leq 200$ and $R_2 = 70$

In the following simulations, we set $\delta = 10^{-3}$ and the 1st carrier eNodeB rate R_1 takes values between 30 and 200 with step of 10, and C2 eNodeB total rate is fixed at $R_2 = 70$. As discussed before, the users' allocated rates are proportional to the users' bids. Real-time application users bid higher than delay-tolerant application users due to their applications nature and the utility proportional fairness policy. Therefore, the pricing which is proportional to the bids is traffic-dependent, i.e. when the demand by users increases, as a result the price increases and vice versa.

In Figure 7, we compare between the shadow price of C1 and C2 eNodeBs when using the proposed RA with joint CA approach with their shadow prices obtained when using the multi-stage RA with CA approach in [9]–[11]. For the RA with joint CA case, we observe that the shadow price of C1 eNodeB is higher than that of C2 eNodeB for $R_1 < 80$ and approximately equal for $80 \leq R_1 \leq 200$ which shows how it is very efficient to use the joint CA approach for the pricing of the user. We also show how the prices decrease with the increase in the eNodeBs total rate. By using this traffic-dependent pricing, the network providers can flatten the traffic specially during peak hours by setting traffic-dependent resource price, which gives an incentive for users to use the network during less traffic hours. On the other hand, for the multi-stage RA with CA approach, we show in Figure 7 the changes in C1 and C2 eNodeBs shadow prices with R_1. When using the multi-stage RA with CA approach, all users are first allocated rates by the macro cell eNodeB, once C1 eNodeB is done allocating its resources C2 eNodeB starts allocating its resources only to the 2nd group users as they are located within its coverage area. Since the pricing method in multi-stage RA with CA approach is not optimal, this explains why the shadow prices of C1 and C2 eNodeBs, in Figure 7, when using
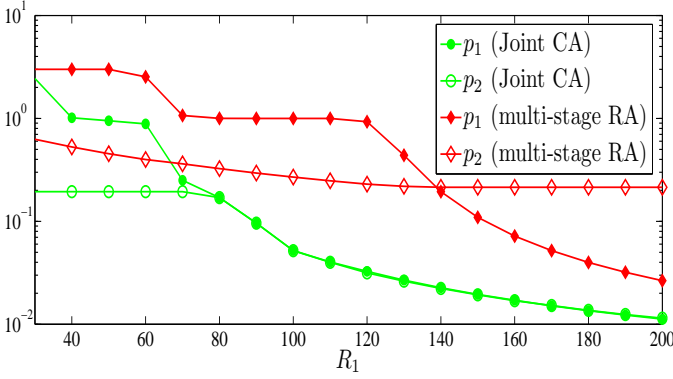
Fig. 7. The 1st carrier shadow price p_1 and 2nd carrier shadow price p_2 for both multi-stage RA with CA and joint RA methods with C1 eNodeB rate $30 < R_1 < 200$ and C2 eNodeB rate $R_2 = 70$.

the proposed RA with joint CA approach are less than their corresponding prices when using the multi-stage RA with CA approach. This shows how the proposed algorithm outperforms the algorithms presented in [9]–[11] as it guarantees that mobile users receive optimal price (minimum) for resources.

VIII. CONCLUSION

In this paper, we introduced a novel resource allocation optimization problem with joint carrier aggregation in cellular networks. We considered mobile users running real-time and delay-tolerant applications with utility proportional fairness allocation policy. We proved that the global optimal solution exists and is tractable for mobile stations with logarithmic and sigmoidal-like utility functions. We presented a novel robust distributed algorithm for allocating resources from different carriers optimally among the mobile users. Our algorithm ensures fairness in the utility percentage achieved by the allocated resources for all users. Therefore, the algorithm gives priority to users with adaptive real-time applications while providing a minimum QoS for all users. In addition, the proposed RA with joint CA algorithm guarantees allocating resources from different carriers with the lowest resource price for the user. We analyzed the convergence of the algorithm with different network traffic densities and presented a robust algorithm that overcomes the fluctuation in allocation during peak traffic hours. We showed through simulations that our algorithm converges to the optimal resource allocation and that the proposed algorithm outperforms the multi-stage RA with CA algorithms presented in [9]–[11] as it guarantees that mobile users receive optimal price for the allocated resources.

REFERENCES

[1] A. Abdel-Hadi and C. Clancy, "An Optimal Resource Allocation with Joint Carrier Aggregation in 4G-LTE," arXiv:1405.6448v1, Accepted in ICNC, 2015.

[2] H. Ekstrom, "QoS control in the 3GPP evolved packet system," *Communications Magazine, IEEE*, vol. 47, pp. 76 –83, february 2009.

[3] M. Iwamura, K. Etemad, M.-H. Fong, R. Nory, and R. Love, "Carrier aggregation framework in 3GPP LTE-advanced [WiMAX/LTE Update]," *IEEE Communications Magazine*, vol. 48, no. 8, pp. 60–67, 2010.

[4] Y. Wang, K. I. Pedersen, T. B. Sørensen, and P. E. Mogensen, "Utility Maximization in LTE-Advanced Systems with Carrier Aggregation," in *VTC Spring*, pp. 1–5, 2011.

[5] G. RP-091440, "Work Item Description: CarrierAggregation for LTE," December 2009.

[6] M. Iwamura, K. Etemad, M.-H. Fong, R. Nory, and R. Love, "Carrier aggregation framework in 3GPP LTE-advanced [WiMAX/LTE Update]," *Communications Magazine, IEEE*, vol. 48, pp. 60–67, August 2010.

[7] PCAST, "Final PCAST Spectrum Report ," July 2012.

[8] R. L. Kurrle, "Resource Allocation for Smart Phones in 4G LTE Advanced Carrier Aggregation," Master Thesis, Virginia Tech, 2012.

[9] H. Shajaiah, A. Abdel-Hadi, and C. Clancy, "Utility Proportional Fairness Resource Allocation with Carrier Aggregation in 4G-LTE," in *Military Communications Conference, MILCOM 2013 - 2013 IEEE*, pp. 412–417, Nov 2013.

[10] H. Shajaiah, A. Khawar, A. Abdel-Hadi, and T. Clancy, "Resource allocation with carrier aggregation in LTE Advanced cellular system sharing spectrum with S-band radar," in *Dynamic Spectrum Access Networks (DYSPAN), 2014 IEEE International Symposium on*, pp. 34–37, April 2014.

[11] H. Shajaiah, A. Abdelhadi, and T. C. Clancy, "A price selective centralized algorithm for resource allocation with carrier aggregation in LTE cellular networks," *arXiv:1408.4151, Accepted in WCNC, 2015*.

[12] A. Abdel-Hadi and C. Clancy, "A utility proportional fairness approach for resource allocation in 4G-LTE," in *Computing, Networking and Communications (ICNC), 2014 International Conference on*, pp. 1034–1040, Feb 2014.

[13] F. Kelly, A. Maulloo, and D. Tan, "Rate control in communication networks: shadow prices, proportional fairness and stability," in *Journal of the Operational Research Society*, vol. 49, 1998.

[14] S. Low, F. Paganini, and J. Doyle, "Internet congestion control," *Control Systems, IEEE*, vol. 22, pp. 28–43, Feb 2002.

[15] S. Low and D. Lapsley, "Optimization flow control. i. basic algorithm and convergence," *Networking, IEEE/ACM Transactions on*, vol. 7, pp. 861–874, Dec 1999.

[16] J. Mo and J. Walrand, "Fair end-to-end window-based congestion control," *Networking, IEEE/ACM Transactions on*, vol. 8, pp. 556–567, Oct 2000.

[17] S. Shenker, "Fundamental design issues for the future internet," *Selected Areas in Communications, IEEE Journal on*, vol. 13, pp. 1176–1188, Sept 1995.

[18] Z. Cao and E. Zegura, "Utility max-min: an application-oriented bandwidth allocation scheme," in *INFOCOM '99. Eighteenth Annual Joint Conference of the IEEE Computer and Communications Societies. Proceedings. IEEE*, vol. 2, pp. 793–801 vol.2, Mar 1999.

[19] S. Sarkar and L. Tassiulas, "Fair allocation of utilities in multirate multicast networks: a framework for unifying diverse fairness objectives," *Automatic Control, IEEE Transactions on*, vol. 47, pp. 931–944, Jun 2002.

[20] A. Abdel-Hadi and C. Clancy, "A robust optimal rate allocation algorithm and pricing policy for hybrid traffic in 4G-LTE," in *Personal Indoor and Mobile Radio Communications (PIMRC), 2013 IEEE 24th International Symposium on*, pp. 2185–2190, Sept 2013.

[21] A. Abdel-Hadi, C. Clancy, and J. Mitola, "A Resource Allocation Algorithm for Multi-Application Users in 4G-LTE," in *MobiCom Workshop*, 2013.

[22] H. Shajaiah, A. Abdel-Hadi, and C. Clancy, "Spectrum sharing between public safety and commercial users in 4G-LTE," in *Computing, Networking and Communications (ICNC), 2014 International Conference on*, pp. 674–679, Feb 2014.

[23] H. Shajaiah, A. Abdelhadi, and C. Clancy, "Multi-Application Resource Allocation with Users Discrimination in Cellular Networks," in *PIMRC*, 2014.

[24] M. Ghorbanzadeh, A. Abdelhadi, and C. Clancy, "A utility proportional fairness radio resource block allocation in cellular networks," *arXiv:1406.2630v1*.

[25] T. Erpek, A. Abdelhadi, and T. C. Clancy, "An optimal application-aware resource block scheduling in LTE," *arXiv:1405.7446v1*.

[26] M. Awad, V. Mahinthan, M. Mehrjoo, X. Shen, and J. W. Mark, "A Dual-Decomposition-Based Resource Allocation for OFDMA Networks With Imperfect CSI," *Vehicular Technology, IEEE Transactions on*, vol. 59, pp. 2394–2403, Jun 2010.

[27] M. Mehrjoo, S. Moazeni, and X. S. Shen, "Resource allocation in OFDMA networks based on interior point methods," *Wireless Communications and Mobile Computing*, vol. 10, no. 11, pp. 1493–1508, 2010.

[28] P. Tejera, W. Utschick, J. Nossek, and G. Bauch, "Rate Balancing in Multiuser MIMO OFDM Systems," *Communications, IEEE Transactions on*, vol. 57, pp. 1370–1380, May 2009.

[29] L. Xu, X. Shen, and J. W. Mark, "Fair resource allocation with guaranteed statistical QoS for multimedia traffic in wideband CDMA cellular network," *Mobile Computing, IEEE Transactions on*, vol. 4, pp. 166–177, March 2005.

[30] M. Mehrjoo, M. Awad, M. Dianati, and X. Shen, "Design of fair weights for heterogeneous traffic scheduling in multichannel wireless networks," *Communications, IEEE Transactions on*, vol. 58, pp. 2892–2902, October 2010.

[31] R. Madan, S. Boyd, and S. Lall, "Fast algorithms for resource allocation in wireless cellular networks," *Networking, IEEE/ACM Transactions on*, vol. 18, pp. 973–984, June 2010.

[32] Y.-B. Lin, T.-H. Chiu, and Y.-T. Su, "Optimal and near-optimal resource allocation algorithms for OFDMA networks," *Wireless Communications, IEEE Transactions on*, vol. 8, pp. 4066–4077, August 2009.

[33] G. Li and H. Liu, "Downlink dynamic resource allocation for multi-cell OFDMA system," in *Signals, Systems and Computers, 2004. Conference Record of the Thirty-Seventh Asilomar Conference on*, vol. 1, pp. 517–521 Vol.1, Nov 2003.

[34] S. Cicalo, V. Tralli, and A. Perez-Neira, "Centralized vs Distributed Resource Allocation in Multi-Cell OFDMA Systems," in *Vehicular Technology Conference (VTC Spring), 2011 IEEE 73rd*, pp. 1–6, May 2011.

[35] M. Dianati, X. Shen, and K. Naik, "Cooperative Fair Scheduling for the Downlink of CDMA Cellular Networks," *Vehicular Technology, IEEE Transactions on*, vol. 56, pp. 1749–1760, July 2007.

[36] P.-L. Tsai, K.-J. Lin, and W.-T. Chen, "Downlink radio resource allocation with Carrier Aggregation in MIMO LTE-advanced systems," in *Communications (ICC), 2014 IEEE International Conference on*, pp. 2332–2337, June 2014.

[37] J.-W. Lee, R. R. Mazumdar, and N. B. Shroff, "Downlink power allocation for multi-class wireless systems," *IEEE/ACM Trans. Netw.*, vol. 13, pp. 854–867, Aug. 2005.

[38] G. Tychogiorgos, A. Gkelias, and K. K. Leung, "Utility-proportional fairness in wireless networks.," in *PIMRC*, pp. 839–844, IEEE, 2012.

[39] S. Boyd and L. Vandenberghe, *Convex Optimization*. New York, NY, USA: Cambridge University Press, 2004.

[40] S. H. Low and D. E. Lapsley, "Optimization flow control, i: Basic algorithm and convergence," *IEEE/ACM Transactions on Networking*, vol. 7, no. 6, pp. 861–874, 1999.